Preclinical evaluation of M30 and M65 ELISAs as biomarkers of drug induced tumor cell death and antitumor activity

Jeffrey Cummings,[1] Cassandra Hodgkinson,[1] Rajesh Odedra,[2] Patrizia Sini,[2] Simon P. Heaton,[2] Kirsten E. Mundt,[2] Tim H. Ward,[1] Robert W. Wilkinson,[2] Jim Growcott,[2] Andrew Hughes,[2] and Caroline Dive[1]

[1]Clinical and Experimental Pharmacology, Paterson Institute for Cancer Research, University of Manchester, Manchester, United Kingdom and [2]Cancer and Infection Research Area, AstraZeneca Pharmaceuticals, Macclesfield, United Kingdom

Abstract

M30 and M65 are ELISAs that detect different circulating forms of cytokeratin 18. Using the aurora kinase inhibitor AZD1152 and the SW620 human colon cancer xenograft, experiments were conducted to qualify preclinically both assays as serologic biomarkers of cell death. Using two different apoptotic markers, the kinetics of cell death induced by AZD1152 was first characterized *in vitro* in three different cell lines and shown to peak 5 to 7 days after drug addition. Treatment of non-tumor-bearing rats with AZD1152 (25 mg/kg) produced no alterations in circulating baseline values of M30 and M65 antigens. In treated, tumor-bearing animals, M30 detected a 2- to 3-fold ($P < 0.05$) increase in plasma antigen levels by day 5 compared with controls. This correlated to a 3-fold increase in the number of apoptotic cells detected on day 5 in SW620 xenografts using immunohistochemistry. By contrast, M65 did not detect a drug-induced increase in circulating antigen levels at day 5. However, M65 plasma levels correlated to changes in tumor growth in control animals ($r^2 = 0.93$; $P < 0.01$) and also followed the magnitude of the temporal effect of AZD1152 on tumor growth. An intermediate but active dose of AZD1152 (12.5 mg/kg) produced a less significant increase in M30 plasma levels at day 5. It was also confirmed that the plasma profiles of M30 and M65 mirrored closely those measured in whole tumor lysates. We conclude that M30 is a pharmacodynamic biomarker of AZD1152-induced apoptosis in the SW620 xenograft model, whereas M65 is a biomarker of therapeutic response. [Mol Cancer Ther 2008;7(3):455–63]

Introduction

The considerable potential of biomarkers to enhance the progress of clinical research and accelerate the pace of drug development is becoming universally recognized (1). Nowhere is this more pertinent than in the complex arena of anticancer drug development, where traditionally the rate of compound attrition is high and success in the clinic is low (2, 3). Accordingly, the Food and Drug Administration, National Cancer Institute, and the Centers for Medicare and Medicaid Services have recently formalized a memorandum of understanding to pursue a collaborative research program known as the Oncology Biomarker Qualification Initiative.

Qualification is the preferred terminology for the evidentiary procedure of causally linking a biomarker to a biological process, pharmacodynamic effect, or clinical endpoint (4, 5). To complete the qualification process can take many years requiring not only retrospective and prospective clinical trials but also large population screening, without any guarantee of eventual success (6–8). Such endeavors can, perhaps, only be successfully negotiated by large-scale cooperative partnerships operating on an national or international basis harnessing the joint resources of the pharmaceutical industry, academia, and national agencies, such as in the case of Oncology Biomarker Qualification Initiative (4, 9, 10). In parallel, academics and the pharmaceutical industry alike are striving to decrease the burden of proof required to qualify a biomarker while maintaining scientific rigor (11). By placing emphasis on mechanistic studies at the preclinical stage, many believe that this approach will increase the prospects of a successful outcome in the clinic after the long qualification cycle (12).

M30 and M65 are relatively newly described sandwich ELISA assays that determine in either plasma or serum different circulating forms of the protein cytokeratin 18 (CK18) and are proposed, based primarily on *in vitro* data, to be surrogate endpoints of different forms of cell death (13, 14). M30 detects a neoepitope mapped to positions 387 to 396 of a 21-kDa fragment of CK18 ($CK18Asp^{396}$ neoepitope) that is only revealed after caspase cleavage of the protein and is postulated as a selective biomarker of apoptotic cell death (15). M65 detects a common epitope present in the full-length protein as well as the 21-kDa caspase cleaved fragment (14) and is thus believed to measure, in addition to apoptosis, intact CK18 that is released from cells undergoing necrosis (16). Our laboratory

Received 9/24/07; revised 11/19/07; accepted 12/14/07.

The costs of publication of this article were defrayed in part by the payment of page charges. This article must therefore be hereby marked *advertisement* in accordance with 18 U.S.C. Section 1734 solely to indicate this fact.

Requests for reprints: Jeffrey Cummings, Clinical and Experimental Pharmacology, Paterson Institute for Cancer Research, University of Manchester, Wilmslow Road, Manchester M20 4BX, United Kingdom. Phone: 44-161-446-3149; Fax: 44-161-446-3109. E-mail: jcummings@picr.man.ac.uk

doi:10.1158/1535-7163.MCT-07-2136

has now validated both assays as fit for purpose in the analysis of plasma/serum collected from subjects entered into clinical trials (17, 18). However, although both ELISAs have now been applied in several clinical trials of anticancer drugs as pharmacodynamic assays (19–21), there have been few formal publications on the qualification of these assays as cell death markers in an *in vivo* model (22). We present the first *in vivo* studies on the preclinical qualification of the M30 and M65 plasma/serum ELISAs as biomarkers of drug-induced tumor cell death and antitumor activity. The study focuses on M30 and M65 responses in an immunodeficient rat bearing a human colorectal cancer xenograft after treatment with the aurora kinase inhibitor AZD1152, which has been shown to have anticancer properties in a preclinical setting (23).

Materials and Methods

Materials

AZD1152 is a dihydrogen phosphate prodrug of a pyrazoloquinazoline aurora kinase inhibitor (AZD1152-hydroxyquinazoline pyrazol anilide) and is converted rapidly to its active metabolite AZD1152-hydroxyquinazoline pyrazol anilide in plasma (23). Both were synthesized by AstraZeneca Pharmaceuticals (24). The M30 and M65 ELISA kits were obtained from PEVIVA. All other chemicals, reagents, and buffers were of the highest grade available commercially and water was purified and deionized in a Millipore Elix 3 system (Millipore).

Cell Line and Tissue Culture

The human tumor cell lines SW620 (colorectal), A549 (lung), and Calu-6 (lung) were obtained from the American Type Culture Collection and cultured as described previously (23).

Induction of Apoptosis *In vitro* after Treatment with AZD1152-Hydroxyquinazoline Pyrazol Anilide Determined by Active Bak and Annexin V Staining

Cells (3,000 per well) were seeded into 96-well plates and exposed to a range of AZD1152-hydroxyquinazoline pyrazol anilide concentrations for 24 h. The compound was then removed. Markers of apoptosis, that is, the activated conformation of Bak (25) and plasma membrane externalization of phosphatidylserine (by positive staining for Annexin V; ref. 26), were determined by high content image analysis screening after a further 48, 96, and 144 h of incubation using the ArrayScan II platform (Cellomics).

Cells were stained for active Bak as follows. After drug incubation, cells were fixed in 2% formaldehyde for 20 min, washed twice with PBS, permeabilized with digitonin (500 μg/mL; Sigma), and stained with mouse anti-Bak antibody (1:100; Calbiochem/Merck Biosciences) for 1 h at room temperature. After washing twice with PBS, cells were incubated with Alexa Fluor 488 goat anti-mouse antibody (1:500; Invitrogen) and Hoechst 33342 stain (1: 5,000; Molecular Probes/Invitrogen) for 30 min at room temperature. Cells were finally washed in PBS and fixed in 1% formaldehyde. The percentage of positively stained cells for active Bak was calculated by the compartmental analysis algorithm (Cellomics).

Annexin V staining was as follows. Annexin V fluorescein conjugate (Invitrogen) and Hoechst 33342 (Invitrogen) were diluted 1:50 from stock with culture medium minus serum to yield a 10× working solution. The working solution was then added to each well to yield a final concentration of 1× and incubated for 15 min at 37°C in an incubator. Immediately after incubation, cells were run on the ArrayScan using the compartmental analysis algorithm (Cellomics).

Antitumor Activity of AZD1152 and Sample Collection for Pharmacodynamic Analysis

Male athymic rats (nude:Hsd Han:RNU-rnu, AstraZeneca) were housed in negative pressure isolators (PFI Systems). Experiments were conducted on 8- to 12-week-old rats in full accordance with the UK Home Office Animal (Scientific Procedures) Act 1986. SW620 tumor xenografts were established by s.c. injecting 200 μL tumor cells (1×10^7 cells mixed 50:50 with Matrigel; Becton and Dickinson) on the flank. Animals were randomized into treatment groups when tumors reached a defined palpable size (0.5-1 cm^3). Thereafter, animals either received AZD1152 (25 mg/kg/d) prepared in Tris (pH 9) or drug vehicle as a daily i.v. bolus via the tail vein on 4 consecutive days. Tumors were measured up to thrice a week with calipers and tumor volumes were calculated using the formula: $[(\text{length} \times \text{width}) \times \sqrt{(\text{length} \times \text{width})} \times (\pi / 6)]$, as described previously (27). Data were plotted as the geometric mean ± SE of tumor volume for each group versus time. Statistical analysis of any change in tumor volume was carried out using a standard Student's two tailed *t* test.

Throughout the antitumor studies, subgroups of animals ($n = 3$ from both AZD1152 and vehicle-treated groups) were sacrificed humanely at multiple time points and blood and whole tumors were collected from each animal for pharmacodynamic analyses. Whole blood was collected using EDTA as anticoagulant and centrifuged at 13,000 rpm for 5 min at 4°C to obtain plasma. Whole tumors were weighed following dissection and either fixed in formalin or snap frozen by immersion in liquid N_2. All samples were stored at -80°C until analysis. Antitumor studies and sample collections were repeated on two separate occasions.

In an additional study, groups of SW620 xenograft-bearing and control animals were treated with either vehicle or 12.5 or 25 mg/kg/d AZD1152 as a continuous infusion over 4 days delivered as described previously (23). Animals ($n = 3$) were humanely sacrificed at different time points and blood was collected from each animal for M30 and M65 analyses. Blood processing was as detailed above.

To assess the potential effect of AZD1152-induced host tissue toxicity on circulating M30 and M65 antigen levels, cohorts of non-tumor-bearing rats were dosed with either drug or vehicle on 4 consecutive days as detailed above. Animals were humanely sacrificed at multiple time points and blood was collected from each animal for pharmacodynamic analysis, with blood processing as above.

Immunohistochemical Detection of Apoptosis in Tumor Using the M30 CytoDEATH Antibody

Formalin-fixed tumors were processed to the paraffin block stage as described previously (23). Tumor tissue sections were cut (3-4 μm thick) and stained for M30 antigen (M30 CytoDEATH, clone M30, IgG2b, mouse; Roche Diagnostics) followed by a one-step horseradish peroxidase–labeled polymer method (Envision; Dakocytomation). Labeling was detected with diaminobenzidine substrate solution (Dakocytomation), and sections were counterstained with Carazzi's hematoxylin. Analysis of immunostaining in tumors sections was determined as the mean percentage of brown staining (n = 6 fields) using a Zeiss KS400 (version 3) image analysis system (Imaging Associates) linked to a Leica DMRB microscope.

Preparation of Tumors for M30 and M65 ELISA Assay

Using a handheld homogenizer (Ultra Turrax), frozen whole tumors were homogenized in RIPA buffer (Sigma) containing the equivalent of 1% of final volume phosphatase 1 and 2 inhibitors (Sigma) and a cocktail of protease inhibitors (Sigma). The volume of RIPA buffer added was calculated as six times the weight of each tumor. Homogenates were vortex mixed to ensure a good suspension and split into two aliquots. All samples were stored on ice for 30 min with further vortex mixing every 5 min. Subsequently, the samples were centrifuged at 13,000 rpm for 5 min at 4°C; supernatants were collected and stored at -80°C until further analysis.

Analysis of Rat Plasma and SW620 Human Xenograft Lysates by M30 and M65 ELISA

The M30 and M65 ELISA kits were used as described previously in detail (17, 18). Before analysis, plasma and tumor lysates, which were stored at -80°C, were allowed to thaw at room temperature. Plasma was analyzed without further sample preparation. Tumor lysates were diluted 1:10; 1:100; 1:1,000, and 1:10,000 with the sample dilution buffer supplied with the M30 and M65 kits. In addition to the normal incubation mixture of 25 μL sample (plasma or tumor lysate) and 75 μL antibody conjugate, 4 μL protein blocking agent HBR plus (Scantibodies Laboratory) was also added to each well.

Results

Kinetics of Induction of Apoptosis *In vitro* after Treatment with AZD1152

Before *in vivo* studies in nude rats bearing the SW620 xenograft, the kinetics of apoptosis induced by AZD1152 was studied in a panel of three cell lines *in vitro* including SW620 cells (see Fig. 1). Two different assays were chosen as markers of apoptosis: detection of the active conformation of Bak (25) and Annexin V binding to phosphatidylserine (26). AZD1152 produced a concentration-dependent increase in both markers over the range of 0.3 to 3 μmol/L. Activated Bak levels peaked at days 3 to 5 (Fig. 1A and C for SW620 and A549, respectively), except at the highest concentrations of AZD1152 in A549 cells (Fig. 1C), whereas apoptosis as measured by Annexin V staining reached a peak at days 5 to 7 (Fig. 1B and D for SW620 and Calu-6, respectively), confirming that Bak activation was the earlier event in the apoptotic cascade.

M30 and M65 Plasma Profiles in Drug-Treated and Control Non-Tumor-Bearing Rats

To determine whether there was potentially a contribution to M30 and M65 circulating antigen levels from host tissue toxicity, plasma collected from drug-treated and vehicle-treated non-tumor-bearing rats were analyzed by M30 and M65 ELISA (see Fig. 2). No significant increases in circulating levels of M30 or M65 antigens above baseline values were detected in the drug-treated animals at any time point studied (days 0, 3, and 5).

Antitumor Activity of AZD1152 in the SW620 Human Colon Cancer Xenograft and Kinetics of the Induction of Apoptosis in the Tumor

The antitumor activity of AZD1152 (after i.v. bolus administration of 25 mg/kg on 4 consecutive days) in two different studies produced a highly consistent effect (e.g., see Fig. 3A). By day 5, control of tumor growth after drug treatment was evident followed by sustained suppression of growth up to day 12, constituting a highly significant tumor growth inhibition at this time point (up to 93%; $P < 0.0005$, Student's t test). After day 12, the tumor entered into a re-growth phase in rats treated with AZD1152 until the termination of the studies on days 16 to 17.

The presence of apoptotic cells in xenografts was detected using the M30 CytoDEATH antibody and immunohistochemistry (Fig. 3B) and quantitated by image analysis (Fig. 3C). M30 CytoDEATH detects a neoepitope on the epithelial protein CK18 ($CK18Asp^{396}$ neoepitope) revealed only after caspase cleavage analogous to the M30 ELISA (15, 16). By day 5, there was a 3-fold increase in M30 reactivity detected in xenograft tissue compared with both day 2 of drug treatment and day 5 of vehicle-treated controls (Fig. 3B and C). Note the increase in large multinucleated cells in AZD1152-treated xenografts (Fig. 3B). Thereafter, a steady decline in the level of apoptosis was recorded in the drug-treated group. In the vehicle-treated controls, the number of M30 positively staining cells detected increased incrementally to a peak after 12 days and then declined.

Correlation between M30 and M65 Antigen Concentrations in Plasma and Pharmacodynamic Effects of AZD1152 on the SW620 Xenograft

Concentration-time profiles generated by M30 and M65 ELISA analysis of plasma were obtained from the two different antitumor studies. In the first study in drug-treated animals, a 3-fold increase in circulating antigen levels was detected by the M30 ELISA at day 5 compared with both day 2 of drug treatment and day 5 of vehicle control (Fig. 4A). This increase paralleled closely the 3-fold increase in apoptosis measured by immunohistochemistry in xenografts 5 days after drug treatment. Circulating levels of M30 antigen were also elevated at day 9 in drug-treated animals compared with day 2 of drug treatment but were not different from control animals at day 9. At day 12, plasma levels of M30 antigen fell in drug-treated animals

compared with controls, corresponding to the time point of maximum antitumor activity (compare Figs. 3A and 4A). By day 16, there was no difference in circulating M30 antigen values between AZD115-treated and control groups.

In the second study, a significant increase (2-fold; $P < 0.01$, Student's t test) in M30 antigen levels in plasma was also recorded at day 5 in drug-treated animals compared with the 30-h time point in the drug-treated group (data not shown). There was also a statistically significant difference between drug-treated and control groups in M30 levels at the day 5 time point ($P < 0.05$, Student's t test), but the magnitude of this difference was less than in the first study. At days 12 and 17, significantly higher levels of M30 antigen were detected in the plasma of control compared with drug-treated animals.

By contrast, the M65 ELISA did not detect a drug-induced increase in circulating antigen levels at the 5-day time point when compared with control animals (Fig. 4B). However, 2- and 4-fold reductions in M65 concentrations in drug-treated animals compared with controls were observed on days 9 and 12 ($P < 0.001$ and 0.05, respectively; Student's t test). The differences in the M65 plasma profiles in controls versus drug-treated animals appeared more indicative of the growth curves obtained during the evaluation of the antitumor activity of AZD1152 in the SW620 xenograft (see Fig. 3A). As in the first study, in a second study, the M65 ELISA did not detect a drug-induced increase in circulating antigen levels at day 5 compared with controls (data not shown) but did consistently record significant reductions in values at the later time points of days 12 and 17 ($P < 0.001$, Student's t test). In addition, the M65 plasma profiles appeared to again follow the trends of the tumor growth curve.

In a separate study, AZD1152 was administered by continuous infusion to rats bearing the SW620 xenograft at doses of 12.5 and 25 mg/kg/d over 4 days and samples were collected for pharmacodynamic analysis. Infusional AZD1152 exhibits a similar level of antitumor activity to i.v. bolus injection (see above), whereas doses close to 12.5 mg/kg/d produce an intermediate level of tumor growth inhibition (55%; $P < 0.05$; ref. 23). Results for the ELISA analysis of plasma samples collected at the key time points of days 2 and 5 are shown in Fig. 4C for the M30 assay and Fig. 4D for the M65 assay. As in the i.v. studies, infusional AZD1152 at 25 mg/kg/d produced a 2-fold increase in M30

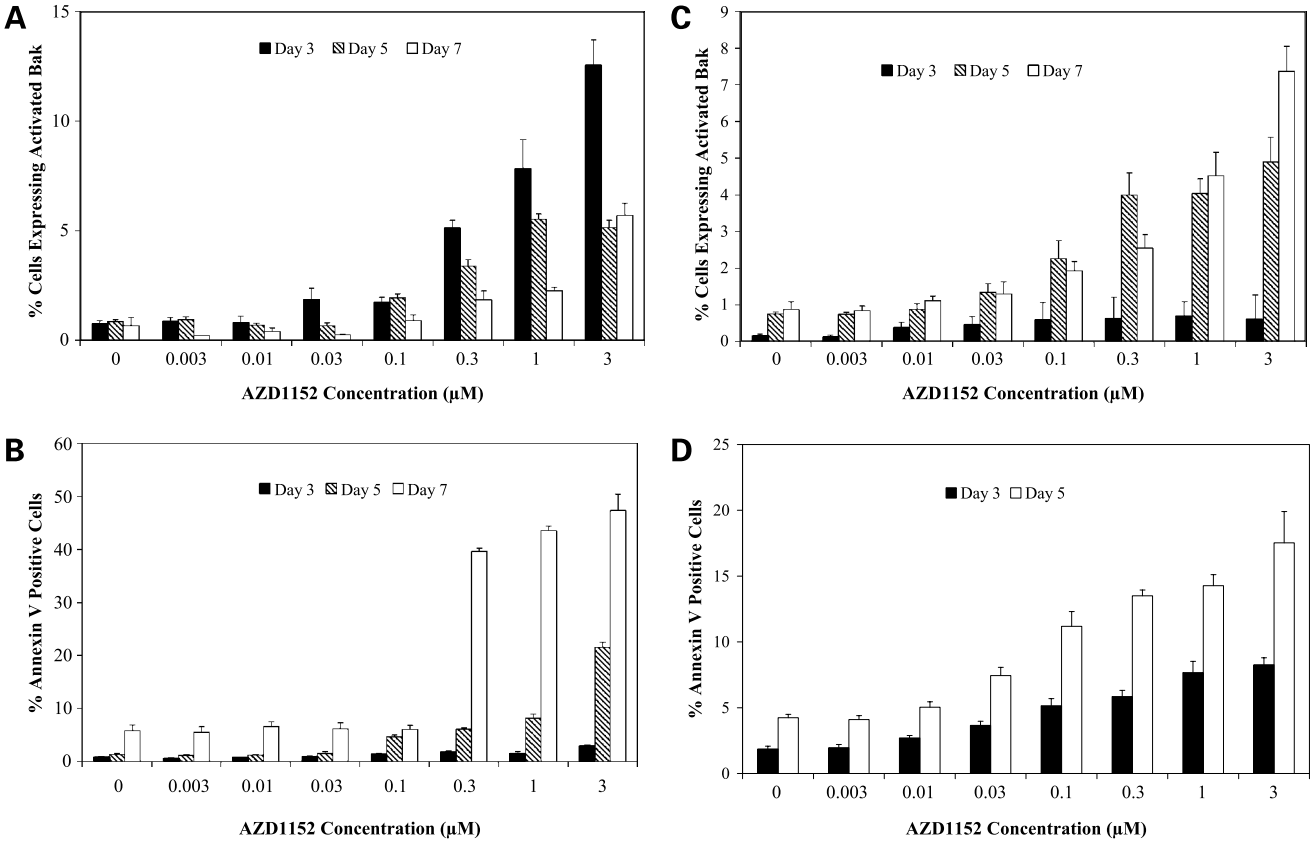

Figure 1. Concentration dependence and time course for the induction of apoptosis in human cancer cell lines *in vitro* after treatment with AZD1152. Cells were seeded into 96-well plates and exposed to a range of AZD1152-hydroxyquinazoline pyrazol anilide concentrations for 24 h. The number of cells staining positive for the activated conformation of Bak or plasma membrane externalization of phosphatidylserine was determined by high content image analysis after a further 2, 4, and 6 d incubation in drug-free medium. **A,** SW620 cells stained for active Bak. **B,** SW620 cells stained for externalization of phosphatidylserine. **C,** A549 cells stained for active Bak. **D,** Calu-6 cells stained for externalization of phosphatidylserine.

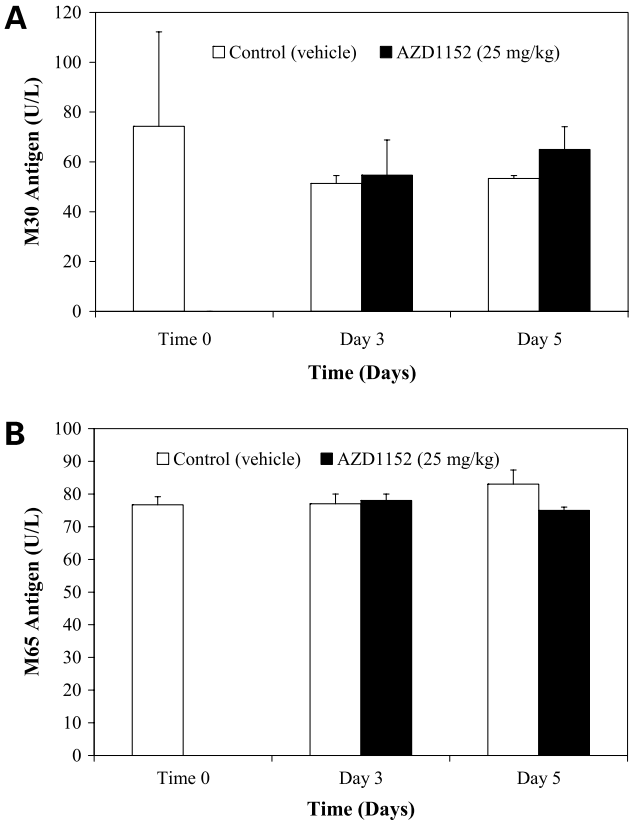

Figure 2. M30 and M65 antigen plasma concentration-time profiles in non-tumor-bearing rats determined after treatment with either AZD1152 or drug vehicle. Rats were treated with AZD1152 (25 mg/kg/d) prepared in Tris (pH 9) or drug vehicle as a daily i.v. bolus via the tail vein on 4 consecutive days. At time 0, days 3 and 5 after the first injection, groups of animals were humanely sacrificed and blood was collected for ELISA analysis of plasma using the M30 (**A**) and M65 (**B**) assays. Columns, mean of three replicate animals; bars, SE.

antigen levels at day 5 compared with controls ($P = 0.005$, Student's t test), whereas no significant increase was recorded with the M65 assay at the same time point. However, at the lower dose level of 12.5 mg/kg, although an increase was detected in M30 antigen concentrations at day 5, this did not reach the level of statistical significance.

Comparison between M30 and M65 Antigen Concentrations in Plasma and in the SW620 Xenograft

M30 and M65 antigen concentrations detected in whole tumor lysates were always 3 to 5 orders of magnitude greater than those detected in plasma. However, if the shape of the profiles in the plasma were compared with those of tumor, they mirrored each other regardless of whether animals were either treated with drug or vehicle. In control animals, plasma and tumor profiles of both M30 and M65 were virtually super imposable (Fig. 5A and *B*). In drug-treated animals, when a 3-fold increase ($P < 0.05$, Student's t test) in M30 levels occurred in the tumor at day 5 compared with 30 h, this was reflected by a 2-fold increase ($P < 0.05$) in the M30 level in plasma at day 5 (Fig. 5C and *D*).

Correlation between M65 Antigen Plasma Profiles and Antitumor Activity of AZD1152

It became evident that M65 plasma levels appeared to correlate more closely with the profile of tumor growth than as a pharmacodynamic biomarker of drug-induced cell death at early time points. In Fig. 6A, M65 plasma levels are plotted against tumor volume for the control

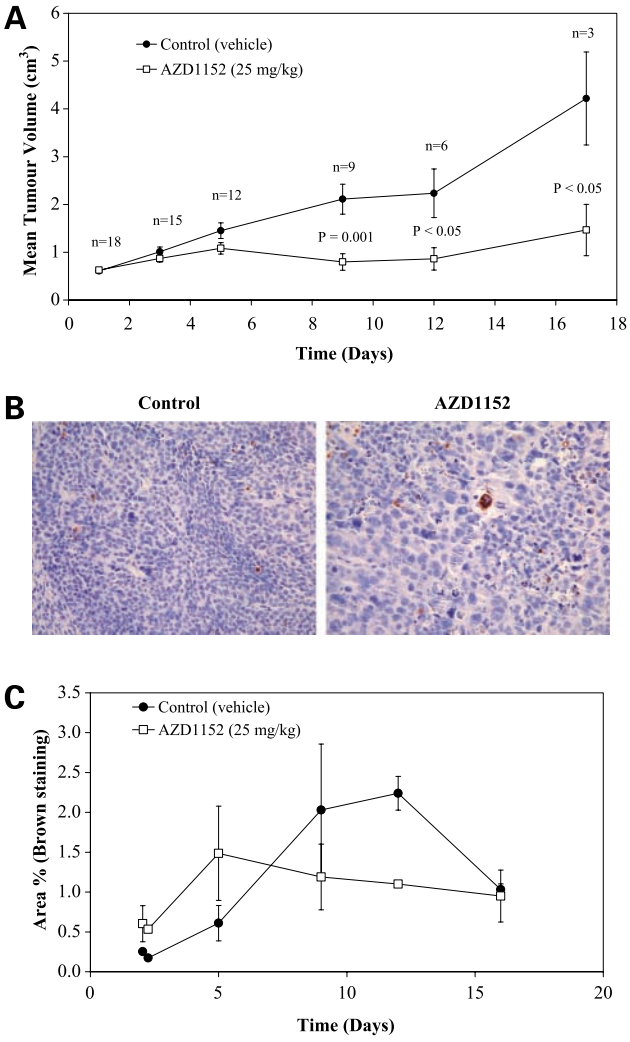

Figure 3. Antitumor activity and pharmacodynamic evaluation of drug-induced apoptosis in the SW620 human colon cancer xenograft after i.v. administration of AZD1152. Rats were treated with AZD1152 (25 mg/kg/d) or drug vehicle as described in Fig. 2. Tumors were then measured up to three times a week with calipers and tumor volumes were calculated. Data are geometric mean ± SE of tumor volume for each time point with the number of animals per group (n; **A**). Significance between drug-treated and control groups is represented at different time points as a P value derived using Student's t test (**A**). At selected time points after treatment with either drug or vehicle, subgroups of rats ($n = 3$) were humanely sacrificed and tumors were collected for analysis. The presence of apoptotic cells in tumor was identified by immunohistochemistry using the M30 CytoDEATH antibody (**B**; data at the day 5 time point) and quantitated by image analysis as mean ± SE percentage of brown staining from six fields (**C**). Note the increase in large multinucleated cells in AZD1152-treated tumors. Magnification, ×40 (**B**).

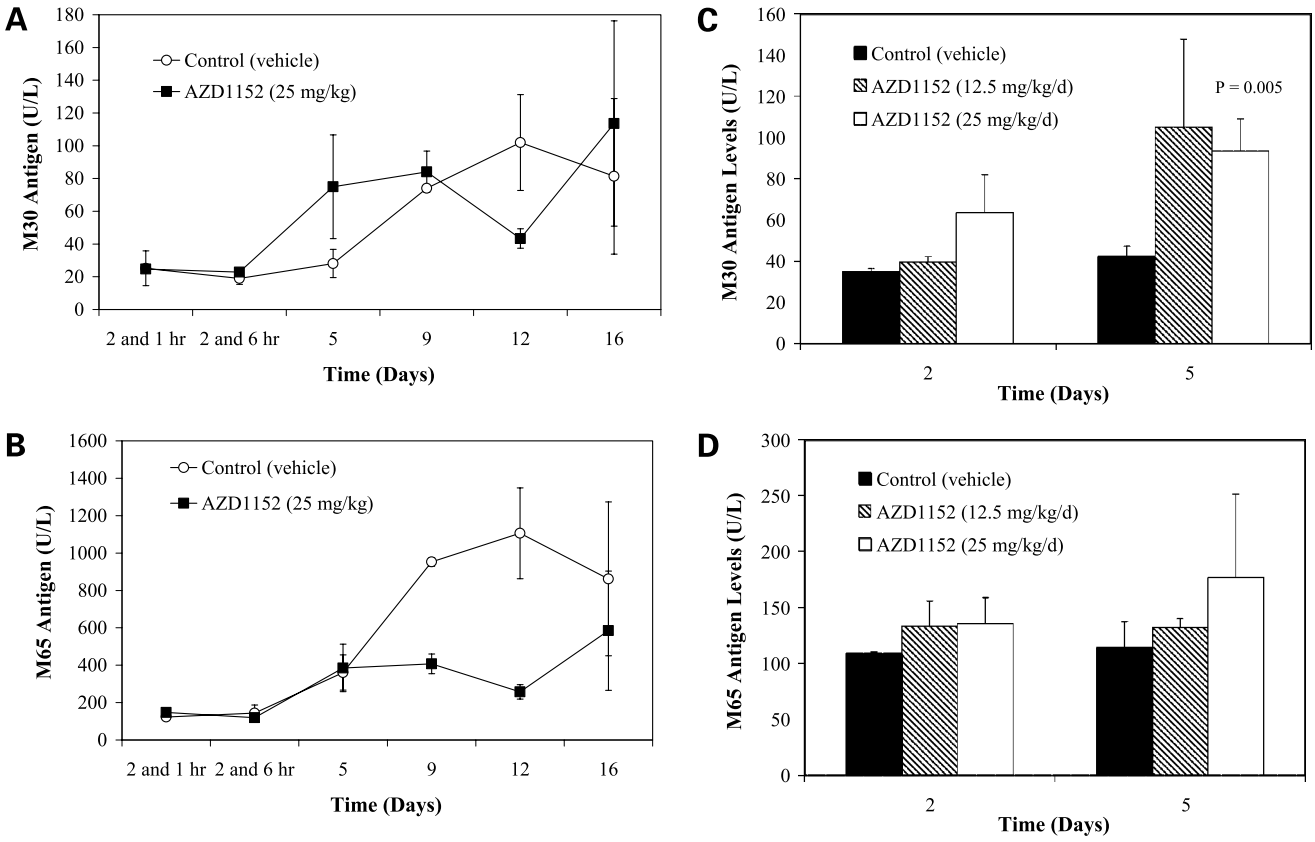

Figure 4. M30 and M65 antigen plasma concentration-time profiles in rats bearing the SW620 xenograft determined after treatment with either AZD1152 or drug vehicle. During the antitumor studies described in Fig. 3, subgroups containing three animals were humanely sacrificed and blood was collected for ELISA analysis of plasma using the M30 assay (**A**) and M65 assay (**B**). In an additional study, AZD1152 was administered as a continuous infusion over 4 d at doses of 12.5 and 25 mg/kg/d and blood samples were collected for analysis by either M30 (**C**) or M65 (**D**). Points, mean of three replicate animals; bars, SE.

group from the second study. Here, a statistically significant regression correlation coefficient (r^2) of 0.93 was obtained ($P < 0.01$, F test), whereas in the first study r^2 was 0.83 ($P < 0.01$; data not shown). Importantly, the M65 plasma profile also closely followed the magnitude of the temporal effect of AZD1152 on tumor growth (Fig. 6B).

Discussion

To preclinically qualify the M30 and M65 ELISAs as pharmacodynamic biomarker assays of tumor cell death, a drug (AZD1152) with a well-characterized mechanism of action (23) was chosen as the cell death–inducing stimulus applied to a drug-sensitive tumor—the human colon cancer xenograft SW620 (28). AZD1152 is a promising new aurora kinase inhibitor, exhibiting selectivity for aurora B, and is currently undergoing clinical trials as an anticancer agent (29). The timescale and nature of the molecular and cellular events that occur in the SW620 xenograft following AZD1152 administration have been reported previously (23). In that study, drug treatment lead to a 40% to 50% inhibition of histone H3 phosphorylation in xenografts after 48 h, resulting in an accumulation of tumor cells displaying a DNA content of ≥4N by day 5. From days 5 to 9, a 2- to 3-fold increase in the number in tumor cells staining positive for active caspase 3 was evident (23). In the present work, it has been confirmed using an additional pharmacodynamic biomarker of cell death (M30 CytoDEATH) that the appearance of high numbers of apoptotic cells in the SW620 xenograft *in vivo* occurs several days (5 days) after treatment with AZD1152. In addition, we now show *in vitro*, in a panel of three different human cell lines including SW620, using two independent markers (activated Bak and Annexin V), that the highest levels of apoptosis induced by AZD1152 are also only detectable several days (5-7 days) after the start of drug incubation.

Our initial *in vivo* analyses were conducted in non-tumor-bearing rats to address the issue of whether drug-induced toxicity to host tissues may contribute to M30 and M65 antigen levels detected in plasma. No significant increases in circulating levels of antigens above baseline values were detected by both assays in these studies, showing that any elevations recorded in xenograft-bearing animals, in both vehicle control and AZD1152-treated rats, are most likely

derived almost exclusively from the tumor. Although AZD1152 does cause extensive but reversible toxicity to the bone marrow (23), neither circulating blood cells nor proliferating chemotherapy-sensitive cells in the bone marrow express CK18 (30); thus, this form of cell death would not be detected by the M30 and M65 assays.

In tumor-bearing animals treated with AZD1152, two major findings emerged. First, the concentration-time profiles of antigens determined by both M30 and M65 ELISA assays in plasma mirrored closely their concentration-time profiles in the tumor. Second, and importantly, changes in circulating levels of CK18 and its caspase cleaved fragments could map precisely to drug-induced perturbations in cellular and biological processes occurring in the tumor, such as apoptosis.

Studies on the preclinical qualification of the M30 ELISA as a selective pharmacodynamic biomarker of tumor cell apoptosis *in vivo* have been severely limited. Most attempts to qualify this assay have relied on either *in vitro* modulation of apoptosis in cancer cell lines (18) or use of tumor slices (22) or have resorted to interpretations of clinical correlations between serum analyses and endpoint data (31, 32). None of these approaches have provided a definite answer to the question of whether plasma M30 profiles accurately reflect events at the level of the tumor. One of the main issues with preclinical studies is that both M30 and M65 ELISAs employ mouse monoclonal antibodies and are subject to interference from endogenous components present in mouse plasma. We minimized this problem by (*a*) using rats and (*b*) using a blocking agent to eliminate false-positive results caused by heterophilic antibodies. Our *in vivo* studies have now shown that the M30 ELISA in plasma is a biomarker of drug-induced apoptosis in tumor correlating with both the amplitude and the timescale of the induction of apoptosis by AZD1152 in the SW620 xenograft when compared against tumor pharmacodynamic biomarkers.

M65 theoretically measures both caspase cleavage (apoptosis) and cellular release of intact CK18 during necrosis and might have been expected to also act as a pharmacodynamic biomarker of tumor cell apoptosis in response to AZD1152 treatment, analogous the M30 assay (14). Nonetheless, our data suggest that M65 is more akin to a marker of tumor growth in control animals as well as a biomarker of therapeutic response in AZD1152-treated animals. Circulating keratins, including CK18, have been recognized for many years as tumor markers in the diagnosis of cancer (33–36). Traditionally, detection of a keratin antigen in serum or plasma, such as tissue polypeptide antigen, MonoTotal (fragments of CK8, CK18, and CK19), tissue polypeptide-specific antigen (CK18 fragments and complexes), or CYFRA21-1 (caspase cleaved CK19), was viewed

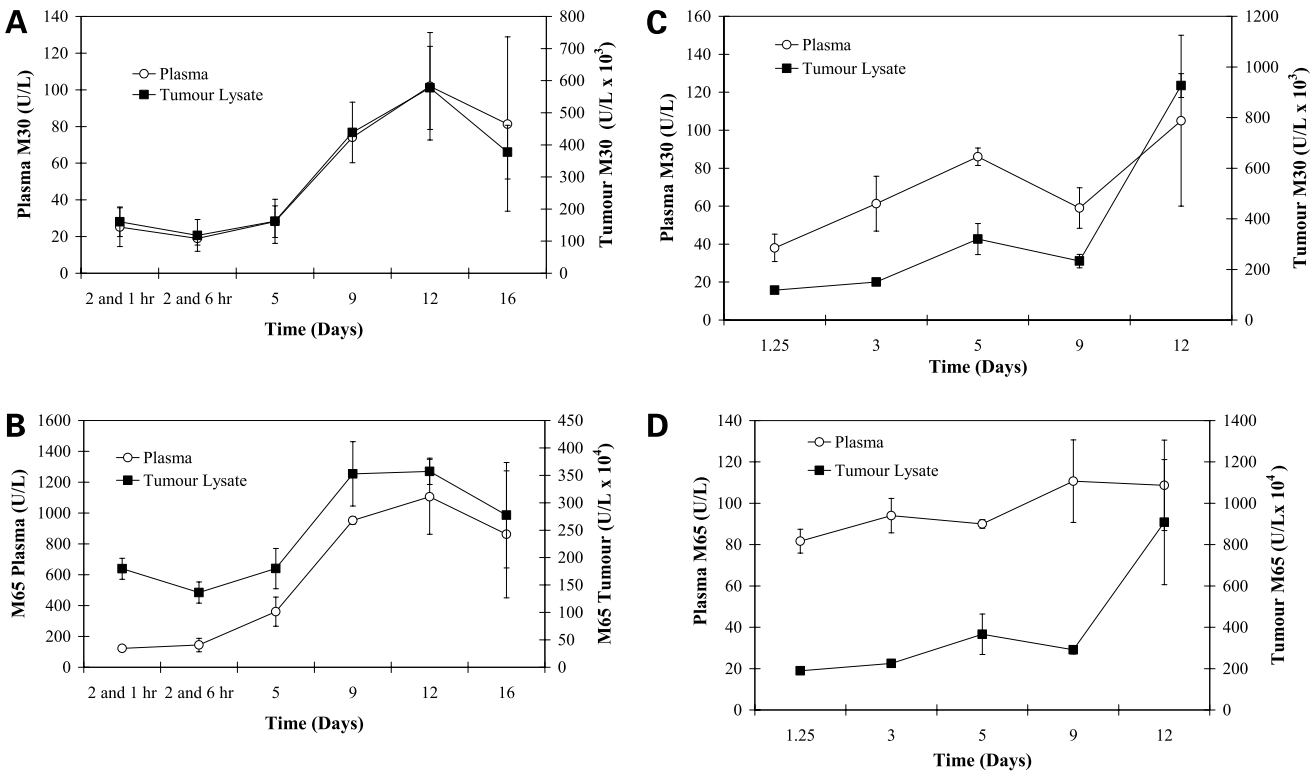

Figure 5. Comparison of M30 and M65 antigen profiles in plasma versus whole tumor lysates in rats bearing the SW620 xenograft determined after treatment with either AZD1152 or drug vehicle. Rats were treated as in Fig. 2. At various different time points, subgroups of three animals were humanely sacrificed and blood and tumor were collected for ELISA analysis using the M30 [**A**, control (antitumor study 1); **C**, drug treated (antitumor study 2)] and M65 assays [**B**, control (antitumor study 1); **D**, drug treated (antitumor study 2)]. Points, mean of three replicate animals; bars, SE.

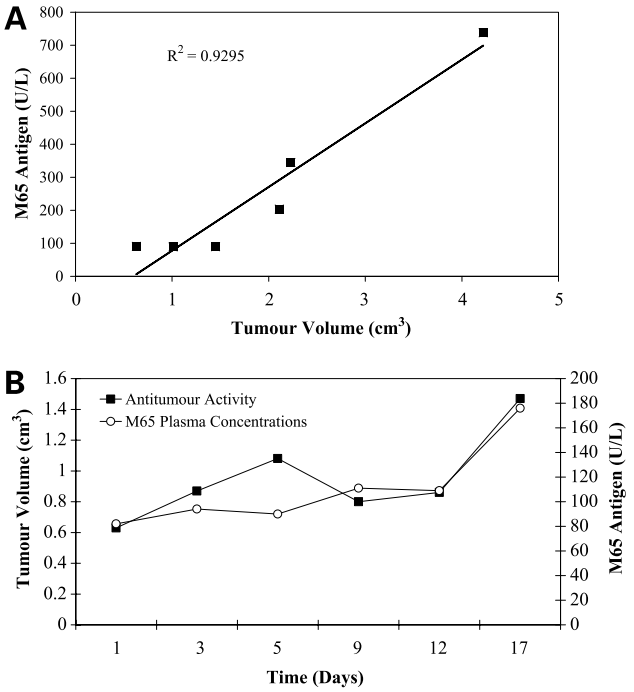

Figure 6. M65 ELISA as a biomarker assay of tumor growth and antitumor activity. **A,** to evaluate the M65 ELISA as a biomarker of tumor growth, tumor volumes measured in the control group of animals were graphed against the concomitant plasma concentrations of M65 antigen determined at the same time points in subgroups of animals. **B,** to evaluate the M65 ELISA as a biomarker of drug response, tumor volumes measured in the AZD1152-treated group of animals were plotted on the same axes as the concomitant plasma concentrations of M65 antigen determined at the same time points in subgroups of animals.

as a passive indicator of bulk tumor burden (35–37). However, it is now believed that the presence of these antigens in the circulation is more representative of active processes taking place in the tumor (14, 16, 19, 38). Indeed, other keratin markers, such as polypeptide antigen and CYFRA21-1, are now also being proposed to be markers of apoptosis rather than tumor volume (14, 39).

Thus, the values generated by the M65 assay in plasma may be more illustrative of tumor growth dynamics, reflecting the balance between cellular proliferation and death, where several oncogenes can drive both processes (40). To support this contention, in our pharmacodynamic analysis in the SW620 human colon cancer xenograft model, we detected higher levels of apoptosis at later time points in control animals compared with the AZD1152-treated animals. Therefore, possibly, as M65 responds as a pharmacodynamic biomarker of cell death at earlier time points in the drug-treated group, the increase in signal is cancelled out in the control group by the greater rate of tumor growth and concomitant increase in cell attrition due to apoptosis. To a lesser extent, the M30 assay may also respond to tumor growth in control animals. This may explain why in the first study compared with the second study, although M30 profiles in plasma both followed closely M30 profiles in tumor and each increased by 2- to 3-fold in value by day 5, the difference between drug-treated values and control values varied from 30% to 300%. Obviously, in cancer patients where the essence of an effective pharmacodynamic biomarker is to detect longitudinal changes in time within individuals, comparisons to a control group are less relevant.

Although our data point to predominately distinct roles for M30 and M65 as biomarkers in our preclinical model, within the context of the clinic, the situation is likely to be even more complex. The M30 ELISA has now also been shown to be a marker of host tissue toxicity in several different clinical conditions including trauma, sepsis (41), chronic liver disease (42), and hepatitis C (43) and in response to liver transplantation (44). The challenge will therefore be to interpret complex biomarker profiles alongside other clinical variables and biochemical measurements.

In summary, we report on three major aspects of preclinical qualification of the M30 and M65 ELISAs as biomarkers. Firstly, we show that plasma profiles generated by both assays mirror closely their profiles in tumor—surrogacy. Secondly, we show that M30 is a more selective pharmacodynamic biomarker of AZD1152-induced apoptosis in the SW620 xenograft model. Thirdly, we show that the M65 plasma correlates to tumor growth but also acts as preferential biomarker of therapeutic response.

References

1. Zerhouni E. Medicine. The NIH roadmap. Science 2003;302:63 – 72.
2. Kamb A, Wee S, Lengauer C. Why is cancer drug discovery so difficult? Nat Rev Drug Discov 2007;6:115 – 20.
3. Kola I, Landis J. Can the pharmaceutical industry reduce attrition rates? Nat Rev Drug Discov 2004;3:711 – 5.
4. Wagner JA, Williams SA, Webster CJ. Biomarkers and surrogate end points for fit-for-purpose development and regulatory evaluation of new drugs. Clin Pharmacol Ther 2007;81:104 – 7.
5. Wagner JA. Overview of biomarkers and surrogate endpoints in drug development. Dis Markers 2002;18:41 – 6.
6. Maruvada P, Srivastava S. Joint National Cancer Institute-Food and Drug Administration workshop on research strategies, study designs, and statistical approaches to biomarker validation for cancer diagnosis and detection. Cancer Epidemiol Biomarkers Prev 2006;15:1078 – 82.
7. Ludwig JA, Weinstein JN. Biomarkers in cancer staging, prognosis and treatment selection. Nat Cancer Rev 2005;5:845 – 56.
8. Pepe MS, Etzioni R, Feng Z, et al. Phases of biomarker development for early detection of cancer. J Natl Cancer Inst 2001;93:1054 – 61.
9. Dalton WS, Friend SH. Cancer biomarkers—an invitation to the table. Science 2006;312:1165 – 8.
10. Bast RC, Jr., Lilja H, Urban N, et al. Translational crossroads for biomarkers. Clin Cancer Res 2005;11:6103 – 8.
11. Williams SA, Slavin DE, Wagner JA, Webster CJ. A cost-effectiveness approach to the qualification and acceptance of biomarkers. Nat Rev Drug Discov 2006;5:897 – 902.
12. Sarker D, Workman P. Pharmacodynamic biomarkers for molecular cancer therapeutics. Adv Cancer Res 2007;96:213 – 68.
13. Hagg M, Biven K, Ueno T, et al. A novel high-through-put assay for screening of pro-apoptotic drugs. Invest New Drugs 2002;20:253 – 9.
14. Kramer G, Erdal H, Mertens HJ, et al. Differentiation between cell death modes using measurements of different soluble forms of extracellular cytokeratin 18. Cancer Res 2004;64:1751 – 6.
15. Leers MP, Kolgen W, Bjorklund V, et al. Immunocytochemical detection and mapping of a cytokeratin 18 neo-epitope exposed during early apoptosis. J Pathol 1999;187:567 – 72.

16. Schutte B, Henfling M, Kolgen W, et al. Keratin 8/18 breakdown and reorganization during apoptosis. Exp Cell Res 2004;297:11 – 26.

17. Cummings J, Ranson M, Lacasse E, et al. Method validation and preliminary qualification of pharmacodynamic biomarkers employed to evaluate the clinical efficacy of an antisense compound (AEG35156) targeted to the X-linked inhibitor of apoptosis protein XIAP. Br J Cancer 2006;95:42 – 8.

18. Cummings J, Ward TH, Lacasse E, et al. Validation of pharmacodynamic assays to evaluate the clinical efficacy of an antisense compound (AEG 35156) targeted to the X-linked inhibitor of apoptosis protein XIAP. Br J Cancer 2005;92:532 – 8.

19. Ueno T, Toi M, Biven K, Bando H, Ogawa T, Linder S. Measurement of an apoptotic product in the sera of breast cancer patients. Eur J Cancer 2003;39:769 – 74.

20. Demiray M, Ulukaya EE, Arslan M, et al. Response to neoadjuvant chemotherapy in breast cancer could be predictable by measuring a novel serum apoptosis product, caspase-cleaved cytokeratin 18: a prospective pilot study. Cancer Invest 2006;24:669 – 76.

21. Ulukaya E, Yilmaztepe A, Akgoz S, Linder S, Karadag M. The levels of caspase-cleaved cytokeratin 18 are elevated in serum from patients with lung cancer and helpful to predict the survival. Lung Cancer 2007;56: 399 – 404.

22. Olofsson MH, Ueno T, Pan Y, et al. Cytokeratin-18 is a useful serum biomarker for early determination of response of breast carcinomas to chemotherapy. Clin Cancer Res 2007;13:3198 – 206.

23. Wilkinson RW, Odedra R, Heaton SP, et al. AZD1152, a selective inhibitor of aurora B kinase, inhibits human tumor xenograft growth by inducing apoptosis. Clin Cancer Res 2007;13:3682 – 8.

24. Mortlock AA, Foote KM, Heron NM, et al. Discovery, synthesis, and *in vivo* activity of a new class of pyrazoloquinazolines as selective inhibitors of aurora B kinase. J Med Chem 2007;50:2213 – 24.

25. Griffiths GJ, Dubrez L, Morgan CP, et al. Cell damage-induced conformational changes of the pro-apoptotic protein Bak *in vivo* precede the onset of apoptosis. J Cell Biol 1999;144:903 – 14.

26. Martin SJ, Reutelingsperger CP, McGahon AJ, et al. Early redistribution of plasma membrane phosphatidylserine is a general feature of apoptosis regardless of the initiating stimulus: inhibition by overexpression of Bcl-2 and Abl. J Exp Med 1995;182:1545 – 56.

27. Wedge SR, Kendrew J, Hennequin LF, et al. AZD2171: a highly potent, orally bioavailable, vascular endothelial growth factor receptor-2 tyrosine kinase inhibitor for the treatment of cancer. Cancer Res 2005;65: 4389 – 400.

28. Goldwasser F, Bae I, Valenti M, Torres K, Pommier Y. Topoisomerase I-related parameters and camptothecin activity in the colon carcinoma cell lines from the National Cancer Institute anticancer screen. Cancer Res 1995;55:2116 – 21.

29. Jackson JR, Patrick DR, Dar MM, Huang PS. Targeted anti-mitotic therapies: can we improve on tubulin agents? Nat Rev Cancer 2007;7: 107 – 17.

30. Linder S, Havelka AM, Ueno T, Shoshan MC. Determining tumor apoptosis and necrosis in patient serum using cytokeratin 18 as a biomarker. Cancer Lett 2004;214:1 – 9.

31. Ueno T, Toi M, Linder S. Detection of epithelial cell death in the body by cytokeratin 18 measurement. Biomed Pharmacother 2005;59 Suppl 2: S359 – 62.

32. Kramer G, Schwarz S, Hagg M, Havelka AM, Linder S. Docetaxel induces apoptosis in hormone refractory prostate carcinomas during multiple treatment cycles. Br J Cancer 2006;94:1592 – 8.

33. Weber K, Osborn M, Moll R, Wiklund B, Luning B. Tissue polypeptide antigen (TPA) is related to the non-epidermal keratins 8, 18 and 19 typical of simple and non-squamous epithelia: re-evaluation of a human tumor marker. EMBO J 1984;3:2707 – 14.

34. Silen A, Wiklund B, Andersson EL, Nilsson S. A novel IRMA and ELISA for quantifying cytokeratin 8 and 18 fragments in the sera of healthy individuals and cancer patients. Scand J Clin Lab Invest 1995;55:153 – 61.

35. Barak V, Goike H, Panaretakis KW, Einarsson R. Clinical utility of cytokeratins as tumor markers. Clin Biochem 2004;37:529 – 40.

36. Seregni E, Coli A, Mazzucca N. Circulating tumour markers in breast cancer. Eur J Nucl Med Mol Imaging 2004;31 Suppl 1:S15 – 22.

37. Brattstrom D, Wagenius G, Sandstrom P, et al. Newly developed assay measuring cytokeratins 8, 18 and 19 in serum is correlated to survival and tumor volume in patients with esophageal carcinoma. Dis Esophagus 2005;18:298 – 303.

38. Einarsson R, Barak V. TPS: a cytokeratin serum tumour marker for effective therapy control of cancer patient with focus on breast cancer. J Clin Ligand Assay 1997;22:348 – 51.

39. Dohmoto K, Hojo S, Fujita J, et al. The role of caspase 3 in producing cytokeratin 19 fragment (CYFRA21-1) in human lung cancer cell lines. Int J Cancer 2001;91:468 – 73.

40. Evan GI, Vousden KH. Proliferation, cell cycle and apoptosis in cancer. Nature 2001;411:342 – 8.

41. Roth GA, Krenn C, Brunner M, et al. Elevated serum levels of epithelial cell apoptosis-specific cytokeratin 18 neoepitope M30 in critically ill patients. Shock 2004;22:218 – 20.

42. Yagmur E, Trautwein C, Leers MP, Gressner AM, Tacke F. Elevated apoptosis-associated cytokeratin 18 fragments ($CK18Asp^{396}$) in serum of patients with chronic liver diseases indicate hepatic and biliary inflammation. Clin Biochem 2007;40:651 – 5.

43. Bantel H, Lugering A, Heidemann J, et al. Detection of apoptotic caspase activation in sera from patients with chronic HCV infection is associated with fibrotic liver injury. Hepatology 2004;40:1078 – 87.

44. Baskin-Bey ES, Washburn K, Feng S, et al. Clinical trial of the pan-caspase inhibitor, IDN-6556, in human liver preservation injury. Am J Transplant 2007;7:218 – 25.